Nematic-Fluctuation-Mediated Superconductivity Revealed by Anisotropic Strain in $\mathrm{Ba(Fe_{1-x}Co_x)_2As_2}$

Jean-Côme Philippe[1] Alexis Lespinas,[1] Jimmy Faria,[1] Anne Forget[2] Dorothée Colson,[2] Sarah Houver,[1] Maximilien Cazayous,[1] Alain Sacuto,[1] Indranil Paul,[1] and Yann Gallais[1,*]

[1]*Université Paris Cité, Matériaux et Phénomènes Quantiques, UMR CNRS 7162, Bâtiment Condorcet, 75205 Paris Cedex 13, France*
[2]*Service de Physique de l'Etat Condensé, DSM/DRECAM/SPEC, CEA Saclay, Gif-sur-Yvette 91191, France*

Anisotropic strain is an external field capable of selectively addressing the role of nematic fluctuations in promoting superconductivity. We demonstrate this using polarization-resolved elasto-Raman scattering by probing the evolution of nematic fluctuations under strain in the normal and superconducting state of the paradigmatic iron-based superconductor $\mathrm{Ba(Fe_{1-x}Co_x)_2As_2}$. In the parent compound $\mathrm{BaFe_2As_2}$ we observe a strain-induced suppression of the nematic susceptibility which follows the expected behavior of an Ising order parameter under a symmetry breaking field. For the superconducting compound, the suppression of the nematic susceptibility correlates with the decrease of the critical temperature T_c, indicating a significant contribution of nematic fluctuations to electron pairing. Our results validate theoretical scenarios of enhanced T_c near a nematic quantum critical point.

In many iron-based superconductors (FeSCs), such as $\mathrm{Ba(Fe_{1-x}Co_x)_2As_2}$ (denoted thereafter as Co:Ba122), superconductivity (SC) occurs around the end point of stripelike antiferromagnetic (AF) and nematic phases, suggesting a link between SC and critical fluctuations associated with the proximity of a nematic or magnetic quantum critical point (QCP) [1–3]. Initially SC was believed to result from magnetic fluctuations [4–6], but following the observation of strong nematic fluctuations through various probes [7–13] nematic degrees of freedom, which break the lattice rotation symmetry while preserving its translation symmetry, have been envisioned as a possible alternative source for the enhancement of the superconducting critical temperature T_c [14–20]. Unfortunately, magnetic and nematic fluctuations are difficult to disentangle in most FeSCs since both phases lie in close proximity. To assess the role of critical nematic fluctuations in enhancing T_c, it is essential to correlate T_c with nematic fluctuations close to the nematic QCP using a stimulus that selectively tunes nematic degrees of freedom.

In this context, anisotropic strain provides an appealing tuning parameter to disentangle the role of magnetic and nematic degrees of freedom in promoting SC because it directly couples to the nematic order parameter ϕ_{nem} provided it has the relevant symmetry, the B_{2g} representation in the case of FeSCs [21–26]. This was demonstrated in the weak-field limit via elastoresistivity measurements which allowed the extraction of the nematic susceptibility χ_{nem} [7]. In the strong field limit, anisotropic strain can also be used as a selective tool to induce or enhance nematic order while leaving the magnetic order comparatively less

affected [25,27,28]. This is because a uniform ($q = 0$) anisotropic strain couples linearly to ϕ_{nem}, but to the finite wave vector Q magnetic order parameter only indirectly via higher orders couplings. Recently, Malinowski *et al.* [29] have revealed in Co:Ba122 a large suppression of T_c under anisotropic strain near the QCP, suggesting an intimate link between SC and nematicity. However, transport measurements cannot probe the nematic fluctuations in the superconducting state, so that the precise link between nematic fluctuations and SC remains to be established in this material.

Here we report an elasto-Raman spectroscopy study on Co:Ba122 establishing a link between nematic fluctuations and T_c under anisotropic strain. In the parent compound Ba122 the effect of strain on nematic fluctuations displays the hallmarks of the susceptibility of an Ising order parameter under a symmetry breaking field. A strong and symmetric reduction of χ_{nem} with strain is observed near the structural transition temperature T_s resulting in a significant suppression of its temperature dependence. For the superconducting compound, a similar reduction of χ_{nem} is observed under strain in both the superconducting and normal states. We further show that the reduction of χ_{nem} scales linearly with T_c, indicating a link between T_c and nematic fluctuations at optimal doping. Our results showcase a dominant role for nematic fluctuations in boosting T_c in Co:Ba122.

Two Co:Ba122 single crystals were investigated. Samples from the same batch were previously studied by transport measurements, from which superconducting T_c, nematic T_s, and AF T_N transition temperatures were

determined, and by Raman scattering under nominally zero strain [9,30–33]. The first crystal is the parent compound, $BaFe_2As_2$ ($x = 0$), which displays a simultaneous magnetic (from paramagnetic to AF) and structural (from tetragonal to orthorhombic) transition at $T_{s/N} = 138$ K and no superconducting state. The second crystal is close to the optimal doping and to the nematic QCP, with $x = 0.07$, $T_c = 24$ K as determined by superconducting quantum interference device magnetometry on the same crystal. It presents no magnetic order and remains tetragonal down to low temperatures. We use an uniaxial piezoelectric cell (CS130 from Razorbill Instruments) to apply both compressive and tensile stress upon a sample glued between two mounting plates. The stress is applied along the long dimension being the [110] direction of the usual two Fe unit cell (that is along the Fe-Fe bonds and denoted x' hereafter), resulting in an anisotropic B_{2g} strain which couples to the B_{2g} nematic order parameter. All the Raman spectra have been corrected for the Bose factor and the instrumental spectral response. They are thus proportional to the imaginary part of the Raman response function $\chi(\omega, T)$. Additional experimental details are given in the Supplemental Material [34] and in Ref. [28], where elasto-Raman phonon spectra obtained on the $x = 0$ sample were already presented.

In the following, we consider an $(x'y'z')$ frame with the x' axis parallel to the applied stress direction. We define $\epsilon_{x'x'}^{nom}$ as the nominal applied strain along the x' direction monitored *in situ* through the measured displacement of the mounting plates. The strain experienced by the sample along the stress direction $\epsilon_{x'x'}$ differs from $\epsilon_{x'x'}^{nom}$ because of the imperfect strain transmission through the epoxy glue [28]. Also due to the finite Poisson ratio, the actual strain is triaxial, and $\epsilon_{x'x'}$ can be decomposed under both two isotropic A_{1g} and one anisotropic B_{2g} components [36]. Throughout the Letter, the data will be shown as a function of $\epsilon_{x'x'}^{nom}$, but the effects of strain transmission will be taken into account when comparing the data on different samples.

All Raman spectra reported here were obtained using crossed polarizations along the principal directions of the 2-Fe unit cell (xy geometry), and thus probe the B_{2g} representation of the D_{4h} point group (see Fig. 1). In this geometry the measured Raman response, denoted $\chi''_{B_{2g}}$ in the following, probes the dynamical nematic fluctuations associated with the order parameter ϕ_{nem}. They can be related to the nematic static susceptibility χ_{nem} through [10]

$$\chi_{nem} = \int_0^\infty \frac{\chi''_{B_{2g}}(\omega)}{\omega} d\omega. \tag{1}$$
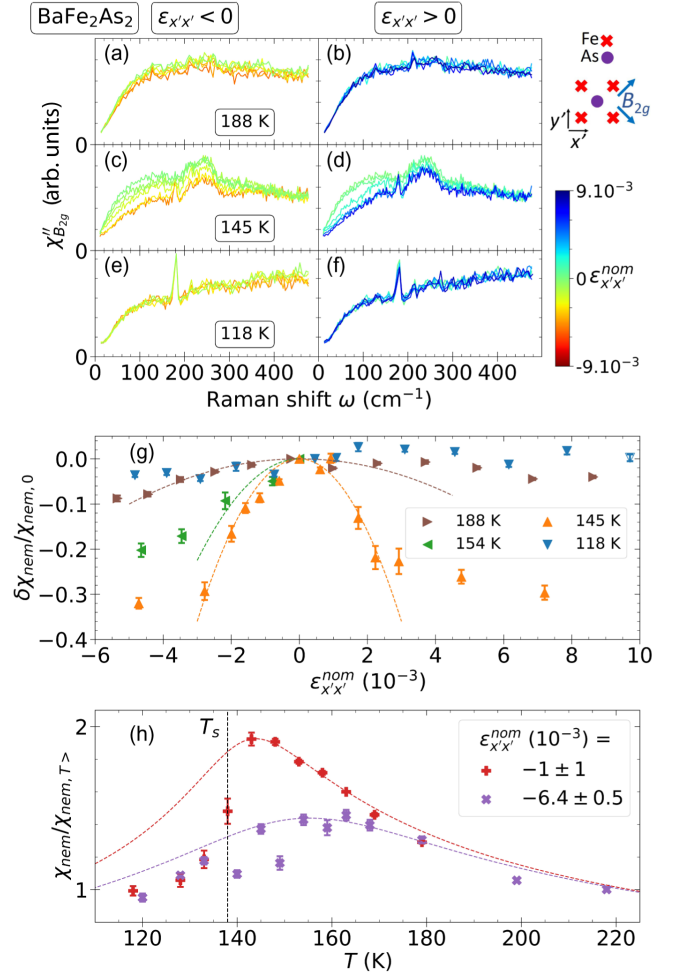

FIG. 1. Strain effect on the nematic (B_{2g}) Raman response for the parent compound $BaFe_2As_2$ ($x = 0$). (a) to (f) Raman response obtained at 188 [(a),(b)], 145 [(c),(d)] and 118 K [(e),(f)], upon negative [(a),(c),(e)] or positive [(b),(d),(f)] strain. The sketch in the upper right displays the directions of the incident and scattered polarizations (blue arrows) with respect to the Fe atom square lattice. (g) Relative variation of χ_{nem} upon strain with respect to the zero strain susceptibility at fixed temperature. No data were obtained at 154 K under tensile strain as the sample broke during the experiment. The dashed lines are guides to the eye using quadratic law [from Eq. (3)]. (h) Temperature dependence of χ_{nem} at fixed strain, renormalized by the high-temperature susceptibility denoted $\chi_{nem,T>}$ (taken here at 220 K under large strain). The dashed lines correspond to the expected theoretical behavior of $\chi_{nem}(T)$ under weak and strong external fields [34]. For (g) and (h), the error bars take into account the uncertainty on the Drude-like low energy extrapolation of the spectra but not the uncertainty related to changes in spot or optical alignment that likely dominate the uncertainty in the temperature dependence [34].

We first present the results concerning the parent compound (Fig. 1). Just above T_s at 145 K, the B_{2g} Raman response is strongly reduced below 300 cm^{-1} both under positive and negative strains. The suppression occurs also at larger temperature (188 K), but is less pronounced. Below T_s at 118 K, $\chi''_{B_{2g}}$ changes very little with strain. At lower temperature, Raman fingerprints of AF spin-density-wave

(SDW) induced gaps indicate a strengthening of the magnetic order under strain (shown in Fig. S6 of the Supplemental Material [34]), in agreement with previous nuclear magnetic resonance measurements [25,32].

With Eq. (1), the decrease of $\chi''_{B_{2g}}$ with strain can be interpreted as a suppression of the nematic fluctuations. Before computing χ_{nem} the experimental spectra were extrapolated down to $\omega = 0$ using a Drude line shape (see Fig. S5 of the Supplemental Material [34]). Because the Raman response does not decrease at high energy [9] we use an upper cut-off frequency $\omega_c = 400\ \mathrm{cm}^{-1}$ in the computation of χ_{nem}, chosen as the upper limit above which no strain effect is observed at all temperatures. The impact of strain on χ_{nem} for four temperatures around T_s is displayed in Fig. 1(g): we define $\chi_{\mathrm{nem},0}$ as the nematic susceptibility at zero strain, and $\delta\chi_{\mathrm{nem}}(\epsilon) = \chi_{\mathrm{nem}}(\epsilon) - \chi_{\mathrm{nem},0}$. Above T_s, at $T = 145$ K, We obtain a clear suppression of χ_{nem} with strain which is symmetric with respect to $\epsilon_{x'x'}^{nom}$. The suppression significantly weakens as T increases. Below T_s, at 118 K, χ_{nem} hardly displays any strain dependence. At 145 K a clear saturation behavior is observed under high tensile and compressive strains. The temperature dependence of χ_{nem} under constant applied strain is depicted in Fig. 1(h). At high strain, the Curie-Weiss-like divergence of $\chi_{\mathrm{nem},0}(T)$ at T_s observed at low strain is strongly suppressed, and the maximum of $\chi_{\mathrm{nem}}(T)$ is shifted to a higher temperature.

The behavior of χ_{nem} under strain can be rationalized in the simple picture of an Ising nematic order parameter coupled to a symmetry breaking field. Using a Landau expansion of the free energy in a mean-field framework in both the nematic and elastic order parameters ϕ_{nem} and ϵ_{xy}, we obtain the following variation of $\delta\chi_{\mathrm{nem}}$ with strain [34]:

$$\frac{\delta\chi_{\mathrm{nem}}}{\chi_{\mathrm{nem},0}} = 3b[\phi_{\mathrm{nem}}^2(\epsilon_{x'x'} = 0) - \phi_{\mathrm{nem}}^2(\epsilon_{x'x'})]\chi_{\mathrm{nem}}(\epsilon_{x'x'}) \quad (2)$$

with $b > 0$ the prefactor of the quartic ϕ_{nem} term in the free energy expression, which we consider strain independent. Restricting ourselves to the low strain regime and to $T > T_s$, to quadratic order in the applied strain we obtain [34]

$$\frac{\delta\chi_{\mathrm{nem}}}{\chi_{\mathrm{nem},0}} \approx -12\left(\frac{C_A}{C_A + \tilde{C}_{66}}\right)^2 b\lambda^2 \chi_{\mathrm{nem},0}^3 \epsilon_{x'x'}^2 \quad (3)$$

with $\lambda > 0$ the nematoelastic coupling constant. $C_A = C_{11} + C_{12}$ and $\tilde{C}_{66}$ are the in-plane isotropic and shear elastic modulus which we define using Voigt notation [34].

Equation (3) qualitatively reproduces two key experimental findings of Fig. 1. First, χ_{nem} should indeed decrease upon strain, following a symmetric quadratic behavior with $\epsilon_{x'x'}$ at low strain. Second, since $\chi_{\mathrm{nem},0}$ increases as T approaches T_s [9,37], the suppression of χ_{nem} with $\epsilon_{x'x'}$ should be larger close to T_s in agreement with our results.
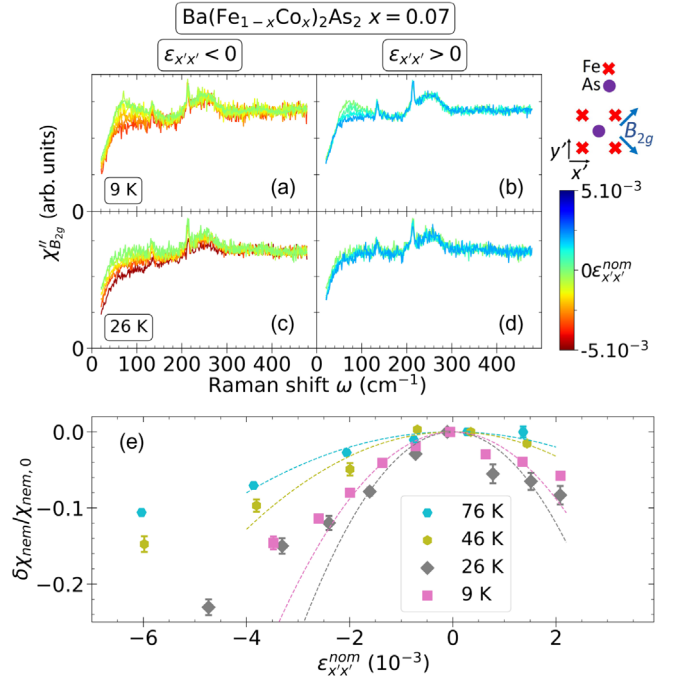

FIG. 2. Strain effect on the nematic (B_{2g}) Raman response for Ba(Fe$_{1-x}$Co$_x$)$_2$As$_2$ ($x = 0.07$). (a)–(d) Raman response obtained at 9 [(a),(b)] and 26 K [(c),(d)], upon negative [(a)–(c)] or positive [(b)–(d)] strain. (e) Relative variation of χ_{nem} upon strain with respect to the zero strain susceptibility at fixed temperature. The dashed lines are guides to the eye obtained by following quadratic laws. The error bars take into account the uncertainty on the low energy extrapolation of the spectra [34]. For the 9 K spectra, the maximum of χ_{nem} occurs at a nominally small compressive strain of approximately -0.5×10^{-3}, whereas for all other probed temperatures for the two samples the maximum is located very close to nominally zero strain. The offset at 9 K is likely due to plastic deformation in the epoxy glue which occurred just before this measurement [42]. Therefore the 9 K data have been shifted by an offset of $+0.5 \times 10^{-3}$ on $\epsilon_{x'x'}^{nom}$.

As shown in Fig. 1(h), this picture also captures the temperature dependence of χ_{nem} under strain, and in particular the upward shift of its maximum at strong strain [34]. Significant deviations below T_s at low strain are likely due to higher order terms in the free energy and/or the onset of AF order, which are not included in the Landau expansion. Overall the behavior of χ_{nem} for the parent compound thus fits very well the expectations of an Ising-nematic order parameter under a symmetry breaking field.

We now move to the results on the doped compound ($x = 0.07$) (Fig. 2) whose composition lies slightly beyond the nematic QCP, located at $x \sim 0.065$ [10,30]. At 9 K, below T_c, the unstrained Raman response shows a relatively broad superconductivity-induced peak centered around 75 cm^{-1}. This was observed before [38,39], and interpreted as a nematic resonance mode where the usual Raman pair-breaking peak at twice the SC gap energy, 2Δ, is replaced by a collective mode below 2Δ because of

significant nematic correlations in the SC state [33,40,41]. Under compressive and tensile strains, the Raman response in the B_{2g} channel is strongly reduced at 9 K and 26 K, indicating a suppression of the nematic fluctuations below and just above T_c. By contrast the spectra in the complementary B_{1g} symmetry channel (displayed in Fig. S4 of the Supplemental Material [34]) hardly show any strain dependence. The strain variation of χ_{nem} [Fig. 2(e)] at different temperatures shows a qualitatively similar behavior as for $x = 0$: a symmetric suppression of χ_{nem} with respect to strain, and a weakening of the strain dependence at higher temperature which follows the behavior of χ_{nem} under zero applied strain [9] as expected from Eq. (3).

We stress that the suppression of χ_{nem} in the superconducting state cannot be simply explained by a reduction of the SC gap magnitude by strain. Indeed in the absence of any nematic correlations, χ_{nem} is just the normal state density of state at the Fermi energy weighted by the B_{2g} Raman vertex. It is therefore independent of the SC gap energy [43], and the suppression of χ_{nem} must be linked to the suppression of nematic fluctuations in the SC state [34]. Moreover, the strain-induced suppression of the SC peak intensity further strengthens the nematic resonance hypothesis: the emergence of the SC peak below T_c is closely linked to the presence of significant nematic correlations in the SC state close to the nematic QCP, as evidenced by the approximate scaling between the SC peak weight and χ_{nem} under strain (see Fig. S2 of the Supplemental Material [34]).

Our results suggest a connection between the suppression of χ_{nem} in the superconducting state and the rapid fall of T_c observed in transport measurements on a similarly doped sample [29]. In the case where SC pairing is promoted by nematic fluctuations as expected near a nematic QCP [16,18], the fall of T_c under strain is rationalized as a consequence of the suppression of these fluctuations.

Within a BCS type of theory [44], with pairing mediated by the nematic fluctuations, we expect $T_c = \Lambda \exp[-1/(N(0)\chi_{\text{nem}})]$ [16–18,45], where Λ is an energy cutoff and $N(0)$ is the density of states at the Fermi energy. Thus, we expect the scaling $\delta T_c \propto \delta\chi_{\text{nem}}$ (see Ref. [34] for a discussion about the range of validity of this scaling).

To further evaluate this point, we plot on Fig. 3 $\delta\chi_{\text{nem}}/\chi_{\text{nem},0}$ as a function of the relative change of T_c under strain, using strain as an implicit parameter. We find that $(\delta T_c/T_c) \propto (\delta\chi_{\text{nem}}/\chi_{\text{nem},0})$ over a significant range of strain: the close correlation between the two quantities clearly supports a nematic-fluctuation-driven SC scenario for Co:Ba122 close to the QCP. We stress that magnetic fluctuations, if anything, are expected to be enhanced by strain [46] as suggested by the enhanced SDW gap observed at $x = 0$ (see Fig. S6 of the Supplemental Material [34]) and also by NMR and neutron diffraction measurements [24,25]. Our elasto-Raman data thus provide
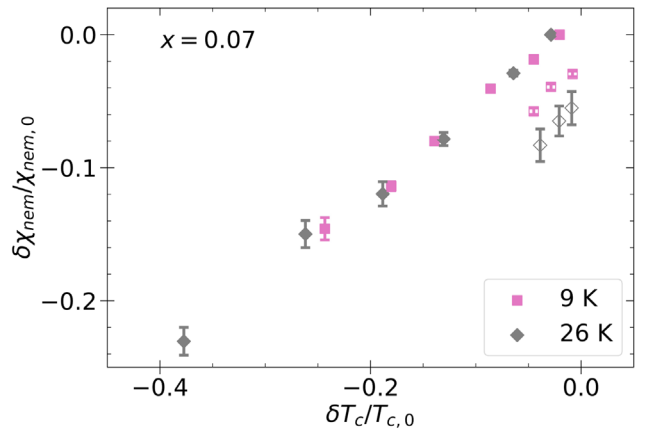

FIG. 3. Scaling between the suppression of χ_{nem} in the superconducting state measured through elasto-Raman spectroscopy and the fall of T_c measured in transport on a crystal with similar doping x. The $T_c(\epsilon_{x'x'}^{\text{nom}})$ data are taken from Ref. [29]. The estimated strain transmission ratios have been taken into account for both datasets [29,34]. The empty symbols stand for the data under positive strain, the filled ones under negative strain. The offset between positive and negative strain data points is partly attributed to uncertainties in the exact location of the zero strain state, but could also possibly reflect an intrinsic asymmetry between tensile and compressive strain [34].

a clear distinction between magnetic and nematic-fluctuation-induced enhancement of T_c in Co:Ba122. We note that in principle the suppression of χ_{nem} with strain could result from the competition between the superconducting and strain-induced nematic orders. However, because nematic order does not significantly reconstruct the Fermi surface, competition between nematic and SC orders is likely weak although its strength and even its sign may depend on the details of the electronic structure [43,47,48]. The weakness of the coupling between both orders is highlighted by the lack of a detectable anomaly in the temperature dependence of χ_{nem} upon crossing T_c as zero strain (see Ref. [34]). The competition scenario is further ruled out by the transport measurements [29], which show that the fall of T_c under strain weakens considerably away from the QCP, favoring a fluctuation effect rather than a mere static competition scenario.

Enhancement of T_c close to a nematic QCP is not universally observed in Fe SC. A particular vexing case is FeSe$_{1-x}$S$_x$ where T_c is even suppressed close to the nematic QCP [49,50]. This was attributed to the coupling to the lattice which cuts off nematic fluctuations, and can significantly quench the expected T_c enhancement found in electron-only models [18,50,51]. The strength of this coupling is embodied in the nematoelastic coupling constant λ between the structural orthorhombic distortion $\epsilon_{B_{2g}}$ to the nematic order parameter ϕ_{nem}. Recently, elastocalorimetric measurements by Ikeda et al. [13] found that λ strongly decreases upon approaching the nematic QCP in Co:Ba122, potentially explaining the observed

nematic-fluctuation-enhanced SC in this compound. The comparison between the two samples in our study can also address this issue since λ appears as a prefactor of the relative variation of nematic susceptibility with strain [Eq. (3)]. However, a quantitative comparison of the two suppressions of χ_{nem} with strain does not support a significant dependence of λ with x (see Fig. S8 of the Supplemental Material [34]). Given this, the origin of the different behaviors of T_c across the nematic QCP in these two Fe SC materials remains an open question.

In conclusion, our elasto-Raman spectroscopy experiments have revealed a strong correlation between superconducting T_c and nematic fluctuations near the nematic QCP of Co:Ba122. We have shown that combining anisotropic strain with Raman scattering which is a sensitive probe of the SC state allows us to decouple the different fluctuation channel contributions to SC pairing. We expect that a similar methodology can be employed to reveal nematic-fluctuation-induced pairing in other materials.

*yann.gallais@u-paris.fr

[1] T. Shibauchi, A. Carrington, and Y. Matsuda, Annu. Rev. Condens. Matter Phys. **5**, 113 (2014).
[2] R. M. Fernandes, A. V. Chubukov, and J. Schmalian, Nat. Phys. **10**, 97 (2014).
[3] H.-H. Kuo, J.-H. Chu, J. C. Palmstrom, S. A. Kivelson, and I. R. Fisher, Science **352**, 958 (2016).
[4] K. Kuroki, S. Onari, R. Arita, H. Usui, Y. Tanaka, H. Kontani, and H. Aoki, Phys. Rev. Lett. **101**, 087004 (2008).
[5] I. I. Mazin, D. J. Singh, M. D. Johannes, and M. H. Du, Phys. Rev. Lett. **101**, 057003 (2008).
[6] D. J. Scalapino, Rev. Mod. Phys. **84**, 1383 (2012).
[7] J.-H. Chu, H.-H. Kuo, J. G. Analytis, and I. R. Fisher, Science **337**, 710 (2012).
[8] M. Yoshizawa, D. Kimura, T. Chiba, A. Ismayil, Y. Nakanishi, K. Kihou, C.-H. Lee, A. Iyo, H. Eisaki, M. Nakajima et al., J. Phys. Soc. Jpn. **81**, 024604 (2012).
[9] Y. Gallais, R. M. Fernandes, I. Paul, L. Chauvière, Y.-X. Yang, M.-A. Méasson, M. Cazayous, A. Sacuto, D. Colson, and A. Forget, Phys. Rev. Lett. **111**, 267001 (2013).
[10] Y. Gallais and I. Paul, C. R. Phys. **17**, 113 (2016).
[11] A. Böhmer, P. Burger, F. Hardy, T. Wolf, P. Schweiss, R. Fromknecht, M. Reinecker, W. Schranz, and C. Meingast, Phys. Rev. Lett. **112**, 047001 (2014).
[12] A. E. Böhmer and C. Meingast, C. R. Phys. **17**, 90 (2016).
[13] M. S. Ikeda, T. Worasaran, E. W. Rosenberg, J. C. Palmstrom, S. A. Kivelson, and I. R. Fisher, Proc. Natl. Acad. Sci. U.S.A. **118**, e2105911118 (2021).
[14] H. Yamase and R. Zeyher, Phys. Rev. B **88**, 180502(R) (2013).
[15] M. A. Metlitski, D. F. Mross, S. Sachdev, and T. Senthil, Phys. Rev. B **91**, 115111 (2015).
[16] S. Lederer, Y. Schattner, E. Berg, and S. A. Kivelson, Phys. Rev. Lett. **114**, 097001 (2015).
[17] T. A. Maier and D. J. Scalapino, Phys. Rev. B **90**, 174510 (2014).
[18] D. Labat and I. Paul, Phys. Rev. B **96**, 195146 (2017).
[19] C. Eckberg, D. J. Campbell, T. Metz, J. Collini, H. Hodovanets, T. Drye, P. Zavalij, M. H. Christensen, R. M. Fernandes, S. Lee et al., Nat. Phys. **16**, 346 (2020).
[20] S. Lederer, E. Berg, and E.-A. Kim, Phys. Rev. Res. **2**, 023122 (2020).
[21] C. Dhital, Z. Yamani, W. Tian, J. Zeretsky, A. S. Sefat, Z. Wang, R. J. Birgeneau, and S. D. Wilson, Phys. Rev. Lett. **108**, 087001 (2012).
[22] C. Dhital, T. Hogan, Z. Yamani, R. J. Birgeneau, W. Tian, M. Matsuda, A. S. Sefat, Z. Wang, and S. D. Wilson, Phys. Rev. B **89**, 214404 (2014).
[23] C. Mirri, A. Dusza, S. Bastelberger, M. Chinotti, J.-H. Chu, H.-H. Kuo, I. R. Fisher, and L. Degiorgi, Phys. Rev. B **93**, 085114 (2016).
[24] D. W. Tam, Y. Song, H. Man, S. C. Cheung, Z. Yin, X. Lu, W. Wang, B. A. Frandsen, L. Liu, Z. Gong et al., Phys. Rev. B **95**, 060505(R) (2017).
[25] T. Kissikov, R. Sarkar, M. Lawson, B. T. Bush, E. I. Timmons, M. A. Tanatar, R. Prozorov, S. L. Bud'ko, P. C. Canfield, R. M. Fernandes et al., Nat. Commun. **9**, 1058 (2018).
[26] H. Pfau, S. D. Chen, M. Hashimoto, N. Gauthier, C. R. Rotundu, J. C. Palmstrom, I. R. Fisher, S.-K. Mo, Z.-X. Shen, and D. Lu, Phys. Rev. B **103**, 165136 (2021).
[27] J. J. Sanchez, P. Malinowski, J. Mutch, J. Liu, J.-W. Kim, P. J. Ryan, and J.-H. Chu, Nat. Mater. **20**, 1519 (2021).
[28] J.-C. Philippe, J. Faria, A. Forget, D. Colson, S. Houver, M. Cazayous, A. Sacuto, and Y. Gallais, Phys. Rev. B **105**, 024518 (2022).
[29] P. Malinowski, Q. Jiang, J. J. Sanchez, J. Mutch, Z. Liu, P. Went, J. Liu, P. J. Ryan, J.-W. Kim, and J.-H. Chu, Nat. Phys. **16**, 1189 (2020).
[30] F. Rullier-Albenque, D. Colson, A. Forget, and H. Alloul, Phys. Rev. Lett. **103**, 057001 (2009).
[31] L. Chauvière, Y. Gallais, M. Cazayous, A. Sacuto, M. A. Méasson, D. Colson, and A. Forget, Phys. Rev. B **80**, 094504 (2009).
[32] L. Chauvière, Y. Gallais, M. Cazayous, M. A. Méasson, A. Sacuto, D. Colson, and A. Forget, Phys. Rev. B **84**, 104508 (2011).
[33] Y. Gallais, I. Paul, L. Chauvière, and J. Schmalian, Phys. Rev. Lett. **116**, 017001 (2016).
[34] See Supplemental Material at http://link.aps.org/supplemental/10.1103/PhysRevLett.129.187002 where [35] is cited for: additional experimental details on Raman experiments and single crystals, the computation of the strain dependence of the nematic order parameter and susceptibility, the impact of strain on the nematic resonance mode, the strain effect on the B_{1g} Raman response, additional details on the extrapolation of the spectra, results about the impact of strain on the magnetic order, and the doping dependence of the nematoelastic coupling.

[35] C. Fujii, S. Simayi, K. Sakano, C. Sasaki, M. Nakamura, Y. Nakanishi, K. Kihou, M. Nakajima, C.-H. Lee, A. Iyo *et al.*, J. Phys. Soc. Jpn. **87,** 074710 (2018).

[36] M. S. Ikeda, T. Worasaran, J. C. Palmstrom, J. A. W. Straquadine, P. Walmsley, and I. R. Fisher, Phys. Rev. B **98,** 245133 (2018).

[37] F. Kretzschmar, T. Böhm, U. Karahasanović, B. Muschler, A. Baum, D. Jost, J. Schmalian, S. Caprara, M. Grilli, C. Di Castro *et al.*, Nat. Phys. **12,** 560 LR18191 (2016).

[38] B. Muschler, W. Prestel, R. Hackl, T. P. Devereaux, J. G. Analytis, J.-H. Chu, and I. R. Fisher, Phys. Rev. B **80,** 180510 (2009).

[39] L. Chauvière, Y. Gallais, M. Cazayous, M. A. Méasson, A. Sacuto, D. Colson, and A. Forget, Phys. Rev. B **82,** 180521(R) (2010).

[40] V. K. Thorsmølle, M. Khodas, Z. P. Yin, C. Zhang, S. V. Carr, P. Dai, and G. Blumberg, Phys. Rev. B **93,** 054515 (2016).

[41] T. Adachi, M. Nakajima, Y. Gallais, S. Miyasaka, and S. Tajima, Phys. Rev. B **101,** 085102 (2020).

[42] M. E. Barber, Ph.D. thesis, University of St Andrews, United Kingdom, 2018.

[43] D. Labat, P. Kotetes, B. M. Andersen, and I. Paul, Phys. Rev. B **101,** 144502 (2020).

[44] J. R. Schrieffer, *Theory of Superconductivity*, Frontiers in Physics (Addison-Wesley Publishing Company, Inc, New York, 1964).

[45] P. J. Hirschfeld, M. M. Korshunov, and I. I. Mazin, Rep. Prog. Phys. **74,** 124508 (2011).

[46] A. Cano and I. Paul, Phys. Rev. B **85,** 155133 (2012).

[47] E.-G. Moon and S. Sachdev, Phys. Rev. B **85** (2012).

[48] X. Chen, S. Maiti, R. M. Fernandes, and P. J. Hirschfeld, Phys. Rev. B **102,** 184512 (2020).

[49] P. Reiss, M. D. Watson, T. K. Kim, A. A. Haghighirad, D. N. Woodruff, M. Bruma, S. J. Clarke, and A. I. Coldea, Phys. Rev. B **96,** 121103 (2017).

[50] S. Chibani, D. Farina, P. Massat, M. Cazayous, A. Sacuto, T. Urata, Y. Tanabe, K. Tanigaki, A. E. Böhmer, P. C. Canfield *et al.*, npj Quantum Mater. **6,** 37 (2021).

[51] P. Reiss, D. Graf, A. A. Haghighirad, W. Knafo, L. Drigo, M. Bristow, A. J. Schofield, and A. I. Coldea, Nat. Phys. **16,** 89 (2020).